Analytical and Bioanalytical Chemistry
https://doi.org/10.1007/s00216-021-03496-0

RESEARCH PAPER

Nitrogen-doped carbon quantum dots fabricated from cellulolytic enzyme lignin and its application to the determination of cytochrome c and trypsin

Chenhui Yin[1] · Ligang Chen[1] · Na Niu[1,2]

Received: 22 April 2021 / Revised: 25 May 2021 / Accepted: 21 June 2021

Abstract

A sensitive and effective strategy for the detection of cytochrome c (Cyt c) and trypsin was developed using biomass nitrogen-doped carbon quantum dots (N-CQDs) as the fluorescence probe. N-CQDs were synthesized through a one-pot hydrothermal method by utilizing cellulolytic enzyme lignin as the carbon source and ammonia as the solvent and nitrogen source. The obtained N-CQDs had good water solubility and stable optical properties. The introduction of nitrogen increased fluorescence quantum yield (QY) to 8.23%, which was almost four times as high as that before nitrogen doping. The N-CQDs were fabricated as a label-free biosensor to detect Cyt c and trypsin. The fluorescence of N-CQDs was quenched with positively charged Cyt c due to electrostatic induction aggregation and static quenching. However, Cyt c tended to be hydrolyzed into small peptides in the presence of trypsin, which caused fluorescence recovery of the N-CQDs/Cyt c complex. A wide linear response range was achieved for Cyt c within 1–50 μM and the developed N-CQDs/Cyt c complex displayed a linear response for trypsin within 0.09–5.4 U/mL. The detection limits were 0.29 μM for Cyt c and 0.013 U/mL for trypsin, respectively. Furthermore, this assay had been applied to Cyt c and trypsin detection in serum samples with the recoveries in the range of 94.6–98.5% and 95.5–102.0%, respectively. The established method was sensitive, selective, easy to operate, and low cost, which proved its potential application in clinical diagnosis.

Keywords Carbon quantum dots · Cytochrome c · Trypsin · Cellulolytic enzyme lignin · Fluorescent sensor

Introduction

Many attempts have been made to develop new detection methods for biological macromolecules to diagnose and treat diseases [1]. Cyt c is generally considered as a protein containing heme peptide fragments and holds great significance in the mitochondrial respiratory chain [2]. In the last few decades, researchers have discovered that Cyt c plays an extremely important role in cell apoptosis [3]. Therefore, the detection of Cyt c, as an important biomarker, could lead to further understanding of certain diseases at the cellular level [4]. Trypsin, a serine protease, could specifically catalyze the hydrolysis of peptide linkage comprising arginine and lysine residues [5, 6]. It is generated by the pancreas and has certain influences on pancreatic exocrine function [7, 8]. Abnormal trypsin levels can induce a variety of pancreatic diseases such as pancreatitis, cystic fibrosis, and cancer [9–11]. Therefore, it is crucial to close monitor Cyt c and trypsin levels in disease diagnosis and treatment.

To date, plenty of methods have been tried to detect Cyt c and trypsin, including electrochemistry [12–14], high-performance liquid chromatography [15], colorimetry [16, 17], and fluorometry [18–21]. In these methods, fluorometric methods have the characteristics of high sensitivity, time-saving, and easy operation. However, among these fluorometric methods, the complicated synthetic steps of some fluorescence

✉ Ligang Chen
analchem@nefu.edu.cn

✉ Na Niu
niuna@nefu.edu.cn

[1] College of Chemistry, Chemical Engineering and Resource Utilization, Key Laboratory of Forest Plant Ecology, Northeast Forestry University, 26 Hexing Road, Harbin 150040, Heilongjiang, China

[2] Key Laboratory of Superlight Materials and Surface Technology, Ministry of Education, College of Materials Science and Chemical Engineering, Harbin Engineering University, Harbin 150001, Heilongjiang, China

Published online: 01 July 2021

probes, high cost, and a large number of chemical reagents, high toxicity, and photobleaching of the probes hinder their practical application.

As fluorescence probes, CQDs are superior to metal nanoclusters and traditional semiconductor quantum dots under some circumstances. They have excellent optical properties, good water dispersibility, and potential application in chemical and biological analysis [22–24]. CQDs can be prepared from various carbon-based raw materials. The precursors for preparing CQDs include large-sized carbon materials and small organic molecules. Large-sized carbon-based materials such as carbon fiber [25], graphene [26], carbon nanotubes [27], graphite rods [28], and coal [29] provide CQDs with regular and highly crystalline structures. The obtained CQDs with small organic molecules such as ethylenediamine [30] and other chemical reagents [31] have the advantages of high purity and abundant surface groups. Relative to certain expensive and toxic chemical reagents, biomass wastes are renewable, low cost, and environmentally friendly. In recent years, biomass CQDs which used agricultural and forestry waste as precursors have become a major research topic. A variety of CQDs has been prepared through different biomass carbon materials such as grass [32], peels [33], leaves [34], and seeds [35]. However, the weak fluorescence hindered their practical application. Therefore, it is urgent to find suitable biomass carbon materials to prepare CQDs. In addition, the fluorescence mechanism and some optimization of synthesis conditions still need to be discussed.

Lignin, a natural polymer composed of phenylpropane units connected by carbon-carbon bonds and ether bonds, is the second-largest biomass resource in the plant kingdom. Compared with the chemical reagent, it has the characteristics of abundant resources, renewable, sustainable, and naturally degradable. Due to its inherent properties, lignin can be transformed into high-value nanoscale fluorescent materials in various ways. In our previous work, cellulolytic enzyme lignin was extracted with ethanol to induce molecular aggregation through π-π polymerization to prepare lignin-based CQDs [36]. However, the obtained CQDs QY is only 1.68–2.47%. Therefore, it is essential to establish a simple and green method to synthesize high-quality lignin-based CQDs.

In this study, biomass N-CQDs were synthesized via a simple hydrothermal method. Cellulolytic enzyme lignin from industrial waste was used as precursor, while ammonia was introduced as the solvent and nitrogen source. The obtained N-CQDs exhibited excellent photoluminescence, which could be served as fluorescence probe. Cyt c incorporated oppositely charged N-CQDs through electrostatic interaction, resulting in fluorescence quenching. Under the proper circumstances, trypsin cleaved the N-CQDs/Cyt c complex into small peptide fragments, leading to fluorescence recovery (Scheme 1). This detection method appeared more selective and sensitive to Cyt c and trypsin. The study not only prepared high-quality fluorescent N-CQDs but also established a strategy for Cyt c and trypsin detection, which had been successfully applied to biological samples.

Material and methods

Reagents and materials

Cellulolytic enzyme lignin was retrieved from the residue of enzymatically hydrolyzed corn stover to produce energy alcohol. Ammonia was supplied by Macklin (Shanghai, China). Proteins such as Cyt c (from horse heart), trypsin (from bovine pancreas), α-glucosidase (α-Glu), and lysozyme (Lyso) were provided by Aladdin (Shanghai, China). Different metal chloride and other biomolecules including KCl, NaCl, L-arginine, L-cysteine, L-alanine, and glucose were provided by Macklin (Shanghai, China). The serum was provided by the Hospital of Northeast Forestry University. The above reagents were of analytical grade and required not to be further purified. Deionized water was used throughout the experiment.

Instrumentation

Fourier transform infrared spectrometer (FTIR) was measured on an FT-IR360 spectrometer (Nicolet, Madison, WI, USA) with potassium bromide pellets. X-ray diffraction (XRD) spectra were obtained by using a TD-3500 spectrometer (Tongda, Dandong, China). The particle size and shape of N-CQDs were recorded by a JEM-2100 transmission electron microscopy (TEM) (JEOL, Tokyo, Japan). UV-Vis absorption spectra (wavenumbers from 200 to 800 nm) were obtained on a TU-1901 spectrophotometer (PERSEE, Beijing, China). The fluorescence spectra of composites were recorded by an F-4600 fluorescence spectrophotometer (Hitachi, Tokyo, Japan). The nanosecond fluorescence lifetime was measured by time-dependent single-photon counting on an FLS-920 instrument (Edinburgh, UK). The X-ray photoelectron spectra (XPS) were conducted on a PHI 5700 ESCA System analyzer (PE, Minnesota, USA).

Synthesis of N-CQDs

The N-CQDs were successfully synthesized via a one-step hydrothermal method. Briefly, 1.6 g cellulolytic enzyme lignin was dissolved in 30 mL ammonia under ultrasonic treatment for 5 min. The mixture was sealed in a hydrothermal autoclave and reacted at 200 °C for 12 h. The dark brown mixture was filtered through a 0.22-μm membrane. Then, the filtrate was dialyzed through a 3500 MWCO dialysis bag. Subsequently, the solid N-CQDs were obtained by freeze-drying the dialysis.

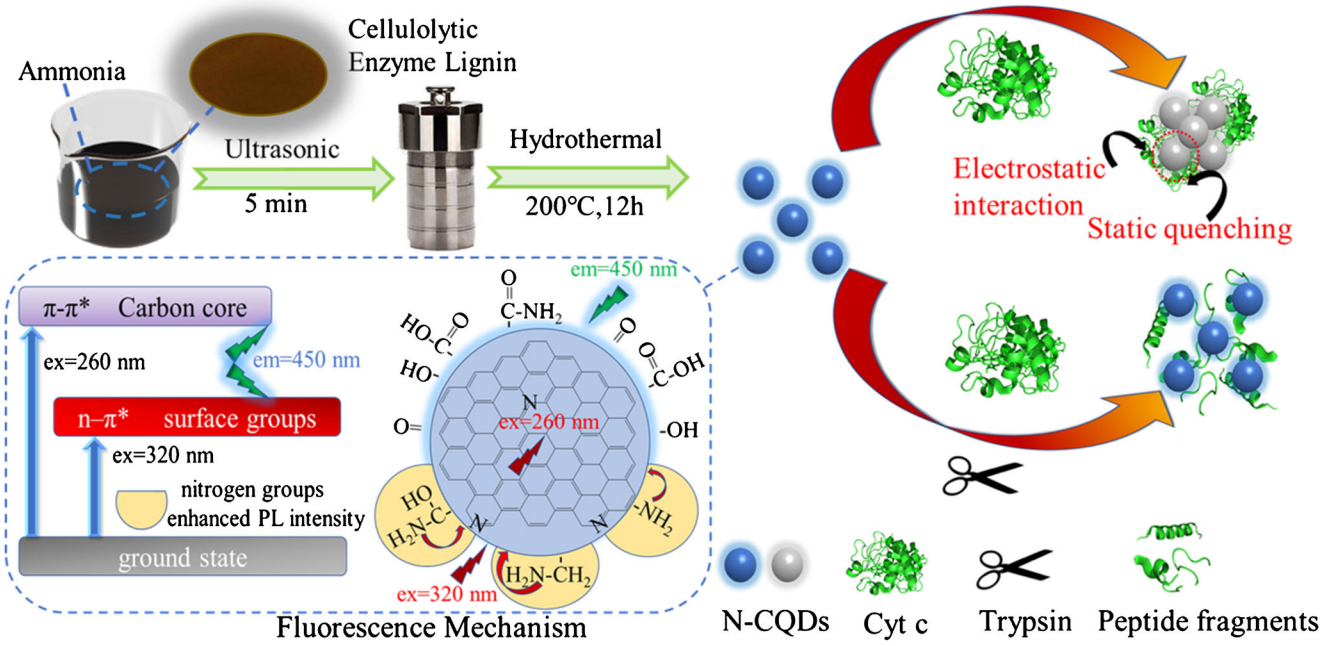

Scheme 1 Schematic illustration of the strategy for Cyt c and trypsin detection

The QY of N-CQDs was calculated according to the equation (Eq. (1)).

$$Q = Q_s(F/F_s)(A_s/A)\left(n^2/n^2{}_s\right) \quad (1)$$

Where n is the refractive index of the solvent, A is the absorbance at appropriate excitation wavelength, F is the luminescence spectra intensity of the emission, and Q is the value of QY. Quinine sulfate in 0.1 M H_2SO_4 (QY=54% at 360 nm excitation) was used as reference whose QY and refractive index was 0.577 and 1.33, respectively.

Fluorescence response of Cyt c

For Cyt c detection, 25 μL various concentrations of the Cyt c and 25 μL N-CQDs (400 μg/mL) were mixed in a calibrated test tube. Then the total volume of mixture was diluted to 250 μL with Tris-HCl buffer (50 mM, pH=8.0). The fluorescence response was recorded under excitation at 320 nm after mixture solution was incubated for 2 min at room temperature.

Sensing trypsin

At first, N-CQDs/Cyt c complex was constructed by the following procedures: 25 μL Cyt c (500 μM), 25 μL N-CQDs (400 μg/mL), and 25 μL Tris-HCl buffer (50 mM, pH=8.0) were mixed and incubated for 2 min at room temperature. Then, 25 μL various concentrations of trypsin and 75 μL N-CQDs/Cyt c complex were added into a calibrated test tube and diluted to 250 μL with Tris-HCl buffer (50 mM, pH=8.0). After incubation at 37 °C for 80 min, the PL intensity changes of different samples were recorded at room temperature.

The real samples detection

The feasibility of the established strategy for Cyt c and trypsin detection in serum samples was studied. Various concentrations of Cyt c or trypsin were added to serum samples and diluted 50 times with Tris-HCl buffer (50 mM, pH=8.0) to prepare the spiked samples.

Results and discussion

Choice of materials

Many methods for Cyt c and trypsin detection have been reported. The low sensitivity of colorimetric methods and low selectivity of electrochemical methods limit their application. For fluorometric methods, metal nanoclusters are costly and traditional semiconductor quantum dots are toxic. As novel fluorescent nanomaterials, CQDs are superior to metal nanoclusters and traditional semiconductor quantum dots under some circumstances. They are almost low toxic and biocompatible, and has unique photoluminescence properties and stability against photobleaching which aroused people's attention in recent years. From the perspective of material synthesis

and environment, it is essential to use cheap, easily available, and environmentally friendly biomass materials to synthesize CQDs.

Cellulolytic enzyme lignin, as a polymer-rich in aromatic structure, is a common industrial waste. They can be used as carbon sources to produce high value-added CQDs. However, the prepared CQDs have the disadvantage of low fluorescence, which hinders their practical application. Heteroatom doping can increase QY and improve optical properties by changing the electronic structure and internal characteristics of N-CQDs. Nitrogen doping can not only effectively improve the fluorescence performance, but also provide potential functional groups for biosensing. In this work, ammonia was used as a nitrogen source. In addition, ammonia played a role in dissolving cellulolytic enzyme lignin.

Optimized synthesis conditions

In this study, ammonia water was used as solvent and nitrogen source. Therefore, the influence of ammonia concentration on QY was investigated. As depicted in Fig. S1 (see Supplementary Information, ESM), ammonia concentration plays a dominant role in the QY of N-CQDs. When the ammonia concentration is less than 2.5 wt%, the QY of N-CQDs increases with the ammonia concentration. It is worth noting that the QY of undoped N-CQDs is only 2.13%. When the ammonia concentration is 2.5 wt%, the QY of N-CQDs reaches 8.23%, which is about four times as much as that before nitrogen doping. It can be inferred that nitrogen doping introduces a new surface state, and the surface nitrogen atoms of N-CQDs capture a large number of electrons and increase their radiation recombination, which improves the fluorescence performance. The QY of N-CQDs no longer increases when the ammonia doping concentration exceeds 2.5 wt%, due to the effective surface traps of N-CQDs becoming saturated. Therefore, 2.5 wt% ammonia was determined as the optimal concentration of ammonia.

Temperature and reaction time influence the QY of N-CQDs as well. When heated for 12 h, the QY of N-CQDs at 200 °C (8.23%) is higher than that of 160 °C (7.31%) and 240 °C (8.16%). Temperature influences the formation of carbon core [37], which can be effectively fluorescent carbon core at an appropriate temperature. When the temperature is too high, the precursor is rapidly dehydrated and aromatized to form a large number of non-fluorescent carbon spheres. In contrast, the precursor is not fully polymerized, and difficult to generate effective fluorescent carbon core. The QY of N-CQDs with a reaction time of 12 h (8.23%) is higher than that of 8 h (7.46%) and 16 h (8.12%) at 200 °C. Therefore, 2.5 wt% ammonia concentration, 200 °C, and 12 h are considered as the optimal condition. The N-CQDs used for characterization and detection later are prepared under optimal conditions.

Characterization of N-CQDs

The morphology and particle size analysis of obtained N-CQDs were characterized by TEM and AFM. As is shown in TEM images (Fig. 1a, b), N-CQDs are evenly distributed in aqueous solution, indicating the obtained N-CQDs have good water solubility. The size distribution ranges from 1.5 to 3.5 nm with an average diameter of 3.0 nm. The lattice distance of 0.21 nm could be observed from the HRTEM images clearly, which is close to the lattice spacing of the graphene (100) crystal plane [38]. The more detailed N-CQDs morphology is characterized through AFM images (Fig. 1c, d), which indicated that the thickness of obtained N-CQDs was 1.1–2.0 nm.

The internal structure and crystal morphology of the synthesized N-CQDs were further characterized by XRD. Figure 2a shows a diffraction peak (2θ) at 22.1°, corresponding to the lattice spacing of C (002) crystal plane. The results indicate that N-CQDs have amorphous carbon structure [39].

The elemental composition and chemical structure were investigated by FT-IR technique and XPS technique. As presented in Fig. 2b, the C-H stretching vibration band of the benzene ring is at 2935 cm^{-1} and 1035 cm^{-1}. The C=C stretching vibration band of the benzene ring skeleton is at 1527 cm^{-1}. It can be inferred that the core of N-CQDs is composed of aromatic skeleton. The O-H stretching vibration band is at 3419 cm^{-1}, and the C=O double bond stretching vibration band is at 1612 cm^{-1}. These results suggest that the surface of N-CQDs consists of hydroxyl and carboxyl groups, which increases the hydrophilic properties of N-CQDs. Notably, the C-O-C absorption peak at 1103 cm^{-1} was significantly weakened along with the 1456 cm^{-1} N-H bending vibration absorption peak. It can be inferred that the C-O-C bond breaks and reorganizes at high temperatures, and nitrogen is successfully doped into the CQDs in the form of amino groups.

More details were obtained by the XPS technique. As shown in Fig. 2c, three strong peaks at 285.2, 399.8, and 532.5eV presented in the full survey XPS spectra can be attributed to C1s, N1s, and O1s characteristic binding energy signals, respectively. Elemental analysis shows that the N-CQDs mainly consist of the three elements of C, N, O, which is estimated to be 81.94% (C), 3.08% (N), and 14.98% (O). The elemental analysis suggests that N-CQDs are successfully doped with nitrogen from ammonia, whose nitrogen content is much more than 1.63% of previously reported alkali lignin-derived N-CQDs [40]. High-resolution C1s spectra (Fig. 2d) show four peaks, corresponding to the C−C/C=C group at 284.8 eV, C-N group at 285.6 eV, C-O group at 286.5 eV, and C=O group at 287.5 eV, respectively. High-resolution O1s spectra (Fig. 2e) show two dominant peaks, corresponding to the O=C group at 531.2 eV and the O-C group at 532.5 eV, respectively. High-resolution N1s spectra

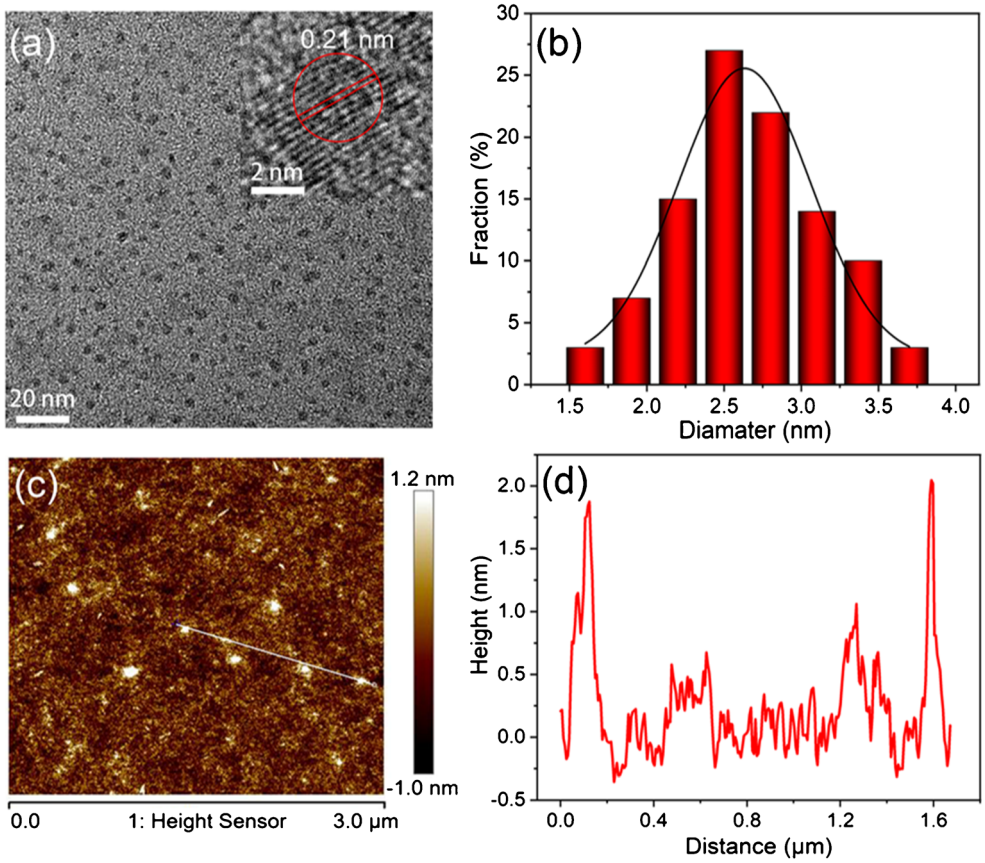

Fig. 1 Morphology analysis of N-CQDs TEM (inset: HRTEM) image of the N-CQDs (**a**), lateral size-distribution diagram (**b**), AFM image of the N-CQDs (**c**), and height profile along the line (**d**)

(Fig. 2f) show three peaks, corresponding to pyridinic-like N at 398.4 eV, the amino group -NH_2 at 399.7 eV, and graphitic-like N at 400.9 eV.

Based on the characterization discussion, it can be inferred that the introduced nitrogen atoms combine with N-CQDs in the form of amino group at the edge sites and conjugate to carbon atoms in the carbon core.

Optical properties and fluorescence mechanism of N-CQDs

N-CQDs aqueous solution exhibited bright blue light at 365-nm UV light (Fig. 3a). According to the UV-Vis spectra in Fig. 3b, there is an obvious absorption peak at 277 nm ascribed to π-π* transition of the aromatic sp^2 domain in the carbon core [41]. Moreover, a narrowly recognized shoulder is found around 320–340 nm, which is possible mainly from n-π* transition of N-CQDs surface groups. Both of them play a vital part in the bright luminescence of N-CQDs due to conjugation between surface groups and carbon core, which could be inferred from fluorescence spectra, FT-IR, and XPS studies. N-CQDs exhibited a unique dual excitation-single emission phenomenon. As is shown in excitation spectra, two excitation peaks at 260 nm and 320 nm are observed under the emission of 452 nm. The excited independent property is observed with the emission peak located at 452 nm when the excitation wavelength ranges from 240 to 350 nm (Fig. 3c). However, N-CQDs have an excitation-independent feature in the range of 360 to 420 nm.

As shown in Fig. S2 (see ESM), N-CQDs show high fluorescence stability after 90 min of continuous irradiation under ultraviolet light, and maintain bright fluorescence in a mild aqueous solution (pH = 6–12), along with low fluorescence intensity under acidic conditions (Fig. 3d). This may be due to the ionization of oxygen-containing groups on the surface of N-CQDs, which leads to the change of electronic states. These features make N-CQDs potential biosensing fluorescence probes for Cyt c and trypsin.

The fluorescence mechanism of N-CQDs was further studied (Fig. 4). The excitation peak at 260 nm could be ascribed to the π-π* transition from amorphous carbon core [42], while that at 320 nm caused by n-π* transition from surface groups. The functional group induces structural deformation to the aromatic carbon core, producing an intermediate state or trap energy level, resulting in a transition of π-intermediate state energy-π* energy level [43]. Therefore, the crystallinity of the carbon core and the surface state energy level play a decisive role in the fluorescence of the CQDs together. The fluorescence QY of undoped CQDs was only 2.13%, but it reached 8.23% after doping with nitrogen. Graphitic-like nitrogen

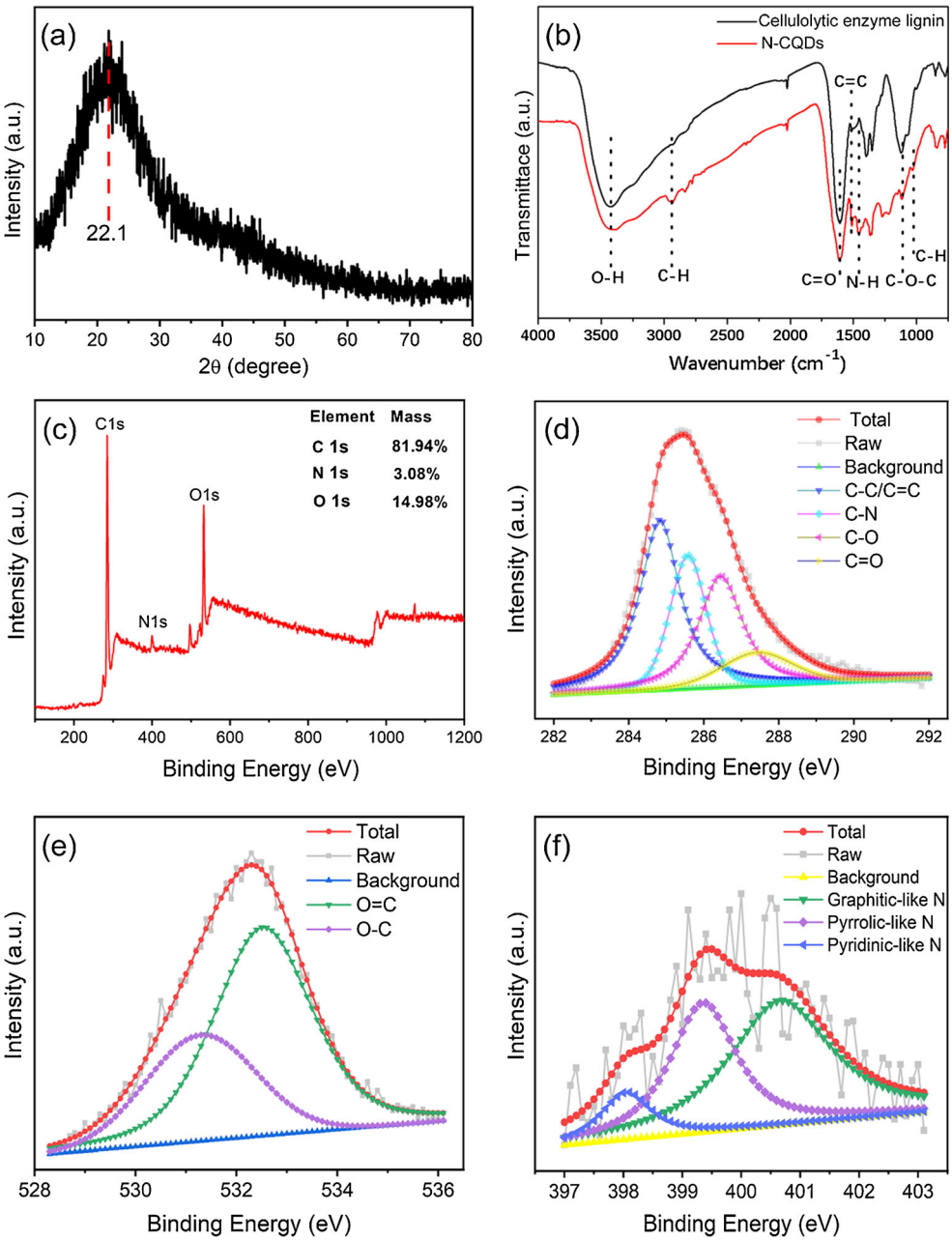

Fig. 2 Chemical analysis of N-CQDs XRD patterns of N-CQDs (**a**), FTIR spectra of cellulolytic enzyme lignin and N-CQDs (**b**), XPS spectra (**c**), high-resolution C 1s (**d**), high-resolution O 1s (**e**), and high-resolution N 1s (**f**)

atoms replace carbon atoms and pyridinic-like nitrogen atoms generate defects. As a result, the fluorescence of N-CQDs is enhanced [44]. Among surface functional groups, nitrogen atoms could change their internal electronic environment in the form of amino by providing electrons to N-CQDs. Moreover, amino can donate electrons to carbonyl groups, resulting in the enlargement of the large conjugate structure of carbonyl groups and sp^2 carbon core [45].

Sensing Cyt c based on N-CQDs

To get the highest sensitivity, pH and reaction time were optimized. In consideration of Cyt c isoelectric point (pI=10.2) and the initial fluorescence of N-CQDs, we investigated the fluorescence of N-CQDs/Cyt c complex at pH=6.8–9.2. As shown in Fig. S3a (see ESM), The quenching extent changes slightly in the pH range of 6.8–9.2. When pH=8.0, the quenching extent of N-CQDs achieved relatively maximum. The reaction time was also taken into consideration and the fluorescence reached a stable value when the reaction time was 2 min (ESM Fig. S3b).

The effect of Cyt c on the fluorescence of N-CQDs was investigated by calculating the relationship between $\ln(F/F_0)$ and concentration of Cyt c under optimal conditions, in which F and F_0 were the PL intensities in the presence and absence of Cyt c. With the increase of Cyt c, the PL intensity of the

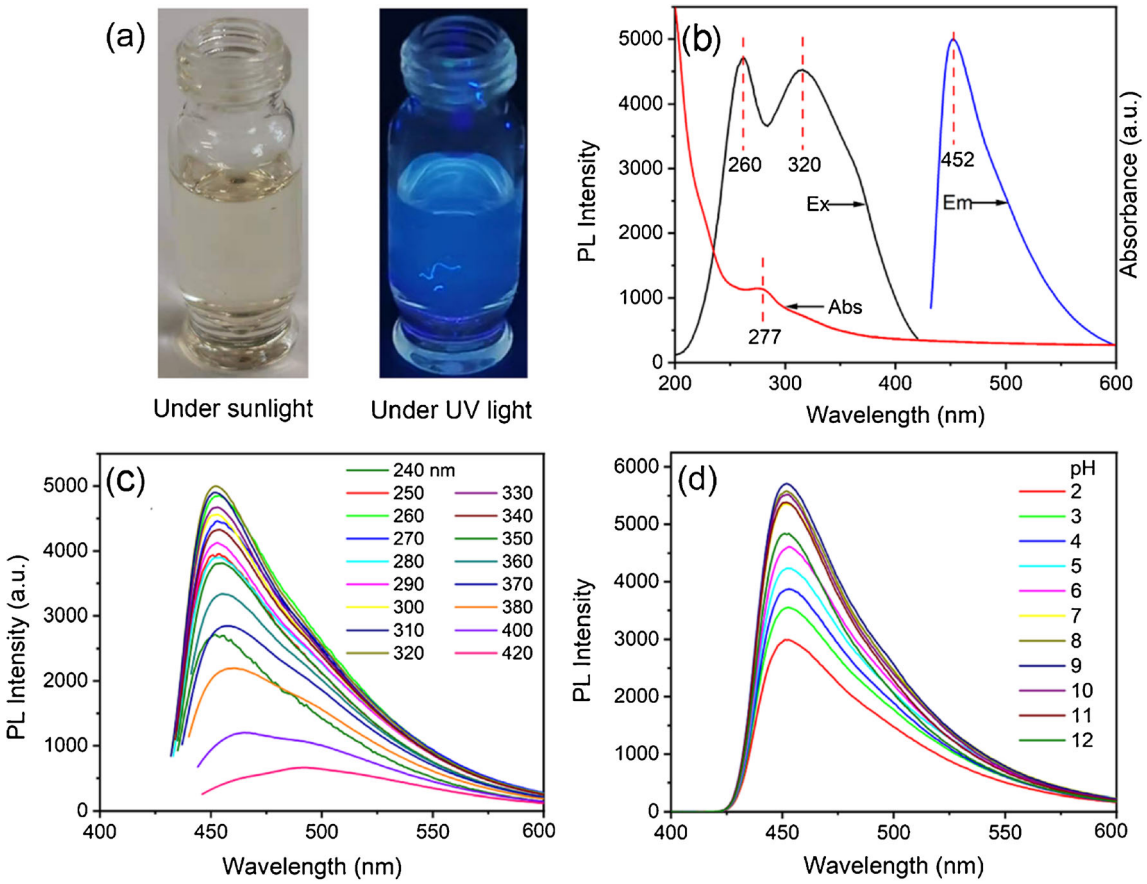

Fig. 3 Optical properties of N-CQDs images of N-CQDs under sunlight and UV light (**a**), the UV-Vis and fluorescence spectra of N-CQDs (**b**), the emission spectra (the excitation wavelength gradually increases from 240 to 420 nm) of N-CQDs in aqueous solution (**c**), and the influence of pH (**d**)

system decreases gradually, accompanied by a redshift of the maximum emission peak (Fig. 5a). A nice linearity was shown from 1 to 50 μM (Fig. 5b) and the regression equation could be expressed as ln (F/F_0) = -0.0327[Cyt c]-0.0665 (R^2 = 0.996). The LOD was determined to be 0.29 μM calculated by three times of signal-to-noise ratio.

Sensing trypsin based on N-CQDs/Cyt c complex

Different influence factors including pH and incubation time were explored to obtain optimal sensing trypsin conditions. Considering that pH had a significant influence on the activity of trypsin, we investigated the fluorescence changes at

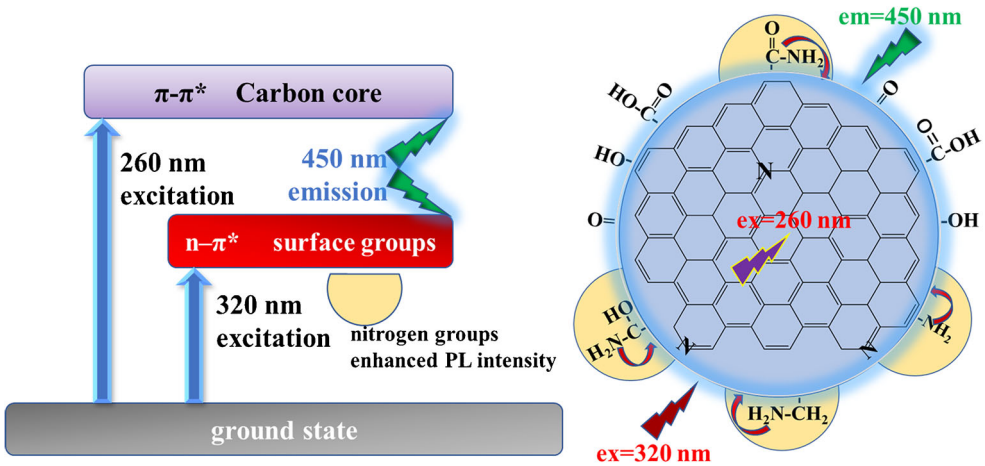

Fig. 4 The fluorescence mechanism of N-CQDs

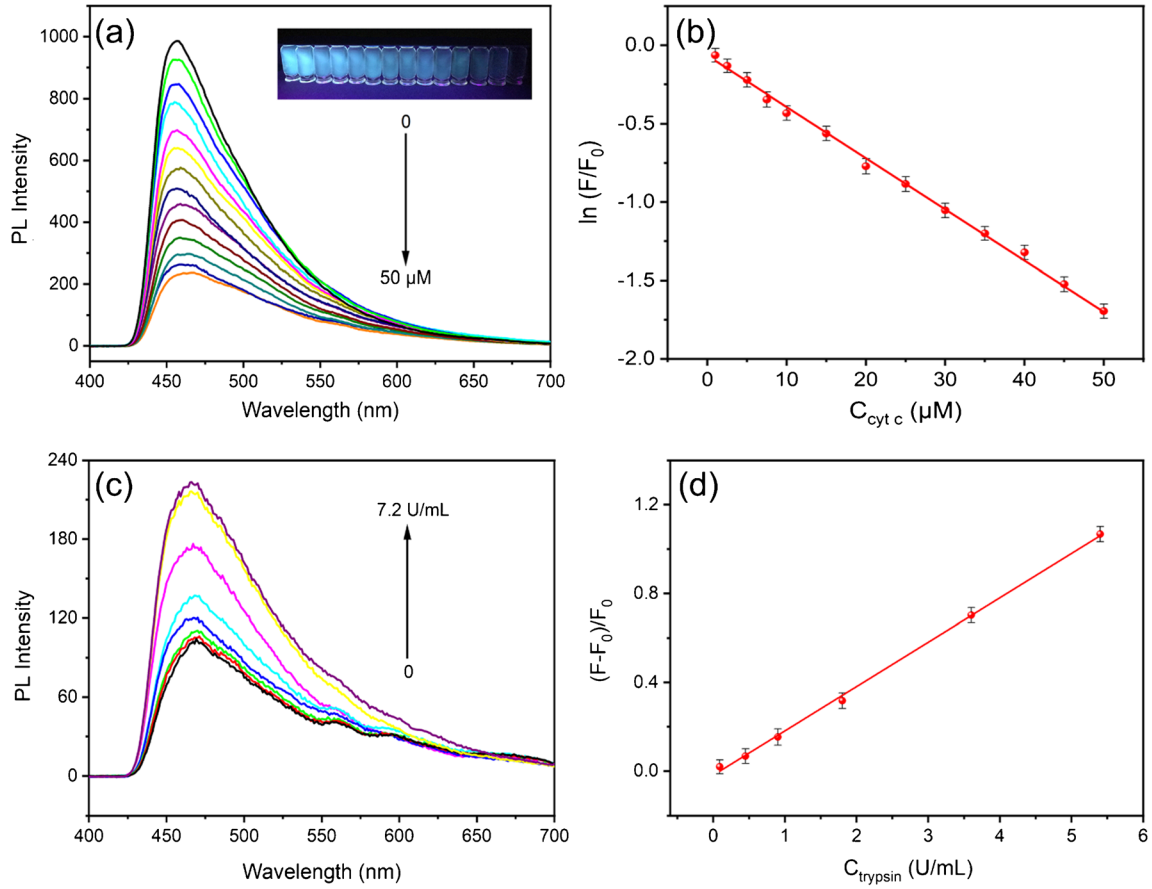

Fig. 5 The fluorescence spectra of N-CQDs at various concentrations of Cyt c (0–50 μM) (**a**), a linear relationship was depicted for Cyt c concentration from 1 to 50 μM by plotting ln (F/F_0) (inset are the images of N-GQDs versus Cyt c under UV light) (**b**), FL spectra of N-CQDs/Cyt c complex with various concentrations of trypsin (**c**), and the linearity between PL intensity ratio of N-CQDs/Cyt c complex and trypsin concentration, where [trypsin] = 0.09, 0.45, 0.9, 1.8, 3.6, 5.4 U/mL (**d**)

pH=6.8–9.2. As shown in Fig. S4a (see ESM), pH 8.0 was determined as the optimal pH condition for this experiment.

Incubation time is the other influencing factor of the assay and N-CQDs/Cyt c complex fluorescence changes at different times were further explored. Enzymatic hydrolysis requires a long reaction time and the fluorescence no longer changed after 80 min (ESM Fig. S4b). Therefore, 80 min was chosen as the optimal incubation time.

With the increase of trypsin, the PL intensity of the N-CQDs/Cyt c complex recovered gradually (Fig. 5c). Good linearity was observed from 0.09 to 5.4 U/mL between the PL intensity ratio of N-CQDs/Cyt c complex and trypsin concentration (Fig. 5d). The regression equation could be expressed as $(F-F_0)/F_0 = 0.20[\text{trypsin}]-0.019$, with an R^2 value of 0.995. The LOD was determined to be 0.013 U/mL calculated by three times of signal-to-noise ratio.

Fluorescence quenching and recovery mechanism

The quenching mechanism of N-CQDs was further explored. First, zeta potential test was conducted (ESM Fig. S5a). N-CQDs have a negative charge with the potential of −9.27 mV at pH=8.0. It is changed to −3.84 mV upon the addition of positively charged Cyt c (3.2 mV). It can be inferred that there is a strong electrostatic interaction between Cyt c and N-CQDs, which may be the cause of fluorescence quenching. Next is to investigate the TEM of N-CQDs after interacting with Cyt c (ESM Fig. S6a). N-CQDs are uniformly distributed in an aqueous solution without Cyt c and turn into aggregates upon adding Cyt c. Consequently, it is not difficult to speculate that the size change of N-CQDs is related to Cyt c, which induces the aggregation of N-CQDs and caused fluorescence quenching. This conclusion is also consistent with the results of zeta potential. Crucially, the fluorescence lifetime of N-CQDs was measured in the presence and absence of Cyt c. Figure S5b (see ESM) shows that the fluorescence lifetime of N-CQDs is 4.4 ns. When Cyt c is added, the fluorescence lifetime of N-CQDs is 4.2 ns. The negligible change in fluorescence lifetime indicates static quenching rather than dynamic quenching. Electron transfer and fluorescence resonance energy transfer are also excluded because they could cause changes in fluorescence lifetime. Finally, the absorption, excitation, and emission spectra were included in the discussion (ESM Fig. S5c). The absorption spectra are from

400 to 600 nm with absorption peaks at 410 nm and 535 nm. The emission spectra of N-CQDs range from 410 to 600 nm with a peak at 452 nm. There is no overlap between them, so the inner filter effect (IFE) could be excluded.

Thermodynamic experiments could also be used to determine the interaction between CQDs and Cyt c. The relative magnitude of enthalpy change (ΔH^0) and entropy change (ΔS^0) of thermodynamic parameters at different temperatures could be calculated according to thermodynamic equations. The thermodynamic equations (Eqs. (2)–(4)) were as follows, where T and R were temperature and universal gas constant (8.314 $J{\cdot}mol^{-1}{\cdot}K^{-1}$), and *K*sv was the equilibrium constant at the corresponding temperature), and ΔH^0, ΔS^0, and ΔG^0 were the entropy change, enthalpy change, and free enthalpy change, respectively.

$$\Delta G^O = -RT\ln K_{SV} \tag{2}$$

$$\Delta G^O = \Delta H^O - \Delta S^O T \tag{3}$$

$$In\ K_{SV} = \frac{\Delta S^O}{R} - \frac{\Delta H^O}{RT} \tag{4}$$

According to the summarized judgment rules [46], it indicated that the interaction mode was electrostatic interaction when $\Delta H^0<0$, $\Delta S^0>0$ (ESM Table S5). This conclusion was consistent with the results discussed above. In conclusion, the possible fluorescence quenching mechanism of N-CQDs versus Cyt c is the effect of electrostatic induction aggregation and static quenching.

The fine quenching ability of Cyt c towards N-CQDs provides the feasibility of constructing an "off-on" mode to detect trypsin by using Cyt c as natural substrates. The fluorescence intensity of N-CQDs/Cyt c complex recovered by addition trypsin. The absorption peaks at 410 nm, 520 nm, and 550 nm were attributed to the heme-Fe (II) in Cyt c. When trypsin was added, the absorption peaks at 520 and 550 nm disappeared, and the absorption peaks blue-shifted from 410 to 400 nm (ESM Fig. S7). The results showed that heme-Fe (II) was released from Cyt c and oxidized to heme-Fe (III) [42], indicating the hydrolysis of Cyt c by trypsin. The zeta potential of N-CQDs/Cyt c complex changed after adding trypsin (ESM Fig. S5a). The substance produced by trypsin hydrolysis of Cyt c was catalytic to hydrogen peroxide, while the original Cyt c had no catalytic activity. This phenomenon was consistent with the literature and illustrated the occurrence of the hydrolysis reaction [47]. Moreover, the TEM image of N-CQDs/Cyt c complex with trypsin implied that trypsin cleaved Cyt c into peptide fragments, leading to the disappearance of aggregation induced quenching (ESM Fig. S6b). All of these revealed that trypsin hydrolyzed Cyt c into peptide fragments, leading to fluorescence recovery.

The selectivity of N-CQDs-based fluorescence probe

Under the optimized experimental conditions, the selectivity of N-CQDs-based fluorescence probe for Cyt c and trypsin was investigated. Different coexisting substances were added to the solution, respectively. It can be seen from Fig. S8a (see ESM) that other substances influenced the fluorescence of N-CQDs negligibly, and only Cyt c had an obvious quenching effect on it. As shown in Fig. S8b (see ESM), the effect of other coexisting substances on the fluorescence of N-CQDs/Cyt c complex was negligible, and only trypsin significantly recovered its fluorescence. These results revealed that the N-CQDs-based fluorescence probe is selective for Cyt c and trypsin.

The real samples detection

We further studied the serum samples to investigate the practicability of the method. To avoid interference from the original sample, the serum sample was diluted 50 times with Tris-HCl buffer. The results are shown in Tables S1 and S2 (see ESM). It can be seen that the average recovery of Cyt c and trypsin ranges from 94.6 to 98.5% and from 95.5 to 102.0%, with relative standard deviation (RSD) lower than 4.5% and 4.9%, respectively. The above results indicate the potential application for Cyt c and trypsin analysis in real samples.

As shown in Tables S3 and S4 (see ESM), this method was compared with other established methods for detecting Cyt c and trypsin. The present method has low sensitivity, simple operation, low cost, environmentally friendly, and fast response time, which is applicable to actual sample analysis.

Conclusions

In the present study, biomass N-CQDs were successfully synthesized via a one-pot hydrothermal method. Fabricating N-CQDs with cellulolytic enzyme lignin as the raw material can convert low-value natural waste into high-value products, which exhibit excellent optical properties. Besides, we have developed a facile and rapid method to selectively detect Cyt c based on N-CQDs and the quenching mechanism has been studied in detail. The effect of electrostatic induction aggregation and static quenching leads to fluorescence quenching. Trypsin cleaved the N-CQDs/Cyt c complex into peptide fragments in some circumstances, resulting in fluorescence recovery. Based on this mechanism, a new strategy was developed and the established method showed good sensitivity, excellent selectivity, and good recovery in actual samples. The biosensor had no need for cumbersome synthesis process of conjugated polymer, no need for labeling, etc. The demonstration of serum samples proved its great potential in practical applications.

Supplementary Information The online version contains supplementary material available at https://doi.org/10.1007/s00216-021-03496-0.

Funding This project was funded by Natural Science Foundation of Heilongjiang Province (B2008001), Heilongjiang Postdoctoral Fund (LBH-Z16009), 111 Project (B20088), Heilongjiang Touyan Innovation Team Program (Tree Genetics and Breeding Innovation Team), and China Postdoctoral Science Foundation (2016M591501, 2017T100218).

Declarations All applicable international, national, and/or institutional guidelines for the collection and use of human blood and serum samples were followed. All biological experiments were approved by the Ethics Committee of Harbin Medical University Cancer Hospital.

Conflict of interest The authors declare no competing interests.

References

1. Lei Z, Jian M, Li X, Wei J, Meng X, Wang Z. Biosensors and bioassays for determination of matrix metalloproteinases: state of the art and recent advances. J Mater Chem B. 2020;8:3261–91.
2. Martinou JC, Desagher S, Antonsson B. Cytochrome c release from mitochondria: all or nothing. Nat Cell Biol. 2000;2:e41–3.
3. Matsuura K, Canfield K, Feng W, Kurokawa M. Metabolic regulation of apoptosis in cancer. Int Rev Cell Mol Biol. 2016;327:43–87.
4. Mesgari F, Beigi SM, Fakhri N, Hosseini M, Aghazadeh M, Ganjali MR. Paper-based chemiluminescence and colorimetric detection of cytochrome c by cobalt hydroxide decorated mesoporous carbon. Microchem J. 2020;157:104991.
5. Liu Y, Zhang F, Xu H, Ma P, Huang Y, Tao S, et al. A novel and simple fluorescent sensor based on AgInZnS QDs for the detection of protamine and trypsin and imaging of cells. Sensor Actuat B-Chem. 2019;294:263–9.
6. Mao G, Peng W, Tian S, Zheng J, Ji X, He Z. Dual-protein visual detection using ratiometric fluorescent probe based on Rox-DNA functionalized CdZnTeS QDs. Sensor Actuat B-Chem. 2018;283:755–60.
7. Zhang S, Chen C, Qin X, Zhang Q, Liu J, Zhu J, et al. Ultrasensitive detection of trypsin activity and inhibitor screening based on the electron transfer between phosphorescence copper nanocluster and cytochrome c. Talanta. 2018;189:92–9.
8. Tabish TA, Pranjol MZI, Karadag I, Horsell DW, Whatmore JL, Zhang S. Influence of luminescent graphene quantum dots on trypsin activity. Int J Nanomedicine. 2018;13:1525–37.
9. Kang OH, Jeong HJ, Kim DK, Choi SC, Kim TH, Nah YH, et al. Trypsin induces tumour necrosis factor-α secretion from a human leukemic mast cell line. Cell Biochem Funct. 2003;21:161–7.
10. Gaber A, Johansson M, Stenman UH, Hotakainen K, Pontén F, Glimelius B, et al. High expression of tumour-associated trypsin inhibitor correlates with liver metastasis and poor prognosis in colorectal cancer. Brit J Cancer. 2009;100:1540–8.
11. Artigas JM, Garcia ME, Faure MR, Gimeno AM. Serum trypsin levels in acute pancreatic and non-pancreatic abdominal conditions. Postgrad Med J. 1981;57:219–22.
12. Pandiaraj M, Sethy NK, Bhargava K, Kameswararao V, Karunakaran C. Designing label-free electrochemical immunosensors for cytochrome c using nanocomposites functionalized screen printed electrodes. Biosens Bioelectron. 2014;54:115–21.
13. Hu Q, Bao Y, Gan S, Zhang Y, Han D, Niu L. Electrochemically controlled grafting of polymers for ultrasensitive electrochemical assay of trypsin activity. Biosens Bioelectron. 2020;165:112358.
14. Ionescu RE, Cosnier S, Marks RS. Protease amperometric sensor. Anal Chem. 2006;78:6327–31.
15. Vestling MM, Murphy CM, Fenselau C. Recognition of trypsin autolysis products by high-performance liquid chromatography and mass spectrometry. Anal Chem. 1990;62:2391–4.
16. Zhang XM, Qin YP, Ye HL, Ma XT, He XW, Li WY, et al. Silicon nanoparticles coated with an epitope-imprinted polymer for fluorometric determination of cytochrome c. Microchim Acta. 2018;185:173.
17. Wang GL, Jin LY, Dong YM, Wu XM, Li ZJ. Intrinsic enzyme mimicking activity of gold nanoclusters upon visible light triggering and its application for colorimetric trypsin detection. Biosens Bioelectron. 2015;64:523–9.
18. Zhang W, He XW, Chen Y, Li WY, Zhang YK. Composite of CdTe quantum dots and molecularly imprinted polymer as a sensing material for cytochrome c. Biosens Bioelectron. 2011;26:2553–8.
19. Guo T, Deng Q, Fang G, Liu C, Huang X, Wang S. Molecularly imprinted upconversion nanoparticles for highly selective and sensitive sensing of cytochrome c. Biosens Bioelectron. 2015;74:498–503.
20. Gu X, Yang G, Zhang G, Zhang D, Zhu D. A new fluorescence turn-on assay for trypsin and inhibitor screening based on graphene oxide. ACS Appl Mater Interfaces. 2011;3:1175–9.
21. Tang B, Yang Y, Wang G, Yao Z, Zhang L, Wu HC. A simple fluorescent probe based on a pyrene derivative for rapid detection of protamine and monitoring of trypsin activity. Org Biomol Chem. 2015;13:8708–12.
22. Feng T, Tao S, Yue D, Zeng Q, Chen W, Yang B. Recent advances in energy conversion applications of carbon dots: from optoelectronic devices to electrocatalysis. Small. 2020;16:2001295.
23. Cao L, Fernando KAS, Liang W, Seilkop A, Veca LM, Sun YP, et al. Carbon dots for energy conversion applications. J Appl Phys. 2019;125:220903.
24. Gao X, Du C, Zhuang Z, Chen W. Carbon quantum dot-based nanoprobes for metal ion detection. J Mater Chem C. 2016;4:6927–45.
25. Peng J, Gao W, Gupta BK, Liu Z, Rebeca RA, Ge L, et al. Graphene quantum dots derived from carbon fibers. Nano Lett. 2012;12:844–9.
26. Li X, Zhu S, Xu B, Ma K, Zhang J, Yang B, et al. Self-assembled graphene quantum dots induced by cytochrome c: a novel biosensor for trypsin with remarkable fluorescence enhancement. Nanoscale. 2013;5:7776–9.
27. Xu X, Ray R, Gu Y, Ploehn HJ, Gearheart L, Raker K, et al. Electrophoretic analysis and purification of fluorescent single-walled carbon nanotube fragments. J Am Chem Soc. 2004;126:12736–7.
28. Liu R, Huang H, Li H, Liu Y, Zhong J, Li Y, et al. Metal nanoparticle/carbon quantum dot composite as a photocatalyst for high-efficiency cyclohexane oxidation. ACS Catal. 2014;4:328–36.
29. Ye R, Xiang C. Lin Jian, Peng Z, Huang K, Yan Z, Cook NP, Samuel ELG, Hwang CC, Ruan G, Ceriotti G, Raji ARO, Martí AA. Tour JM Coal as an abundant source of graphene quantum dots Nat Commun. 2013;4:2943.
30. Huang S, Yang E, Yao J, Liu Y, Xiao Q. Carbon dots doped with nitrogen and boron as ultrasensitive fluorescent probes for determination of α-glucosidase activity and its inhibitors in water samples and living cells. Microchim Acta. 2018;185:394.
31. Dadkhah S, Mehdinia A, Jabbari A, Manbohi A. Rapid and sensitive fluorescence and smartphone dual-mode detection of dopamine

based on nitrogen-boron co-doped carbon quantum dots. Microchim Acta. 2020;187:569.
32. Liu S, Tian J, Wang L, Zhang Y, Qin X, Luo Y, et al. Hydrothermal treatment of grass: a low-cost, green route to nitrogen-doped, carbon-rich, photoluminescent polymer nanodots as an effective fluorescent sensing platform for label-free detection of Cu (II) Ions. Adv Mater. 2012;24:2037–41.
33. Lu W, Qin X, Liu S, Chang G, Zhang Y, Luo Y, et al. Economical, green synthesis of fluorescent carbon nanoparticles and their use as probes for sensitive and selective detection of mercury (II) ions. Anal Chem. 2012;84:5351–7.
34. Kumawat MK, Thakur M, Gurung RB, Srivastava R. Graphene quantum dots from Mangifera indica: application in near infrared bioimaging and intracellular nanothermometry. ACS Sustain Chem Eng. 2017;5:1382–91.
35. Qu F, Pei H, Kong R, Zhu S, Xia L. Novel turn-on fluorescent detection of alkaline phosphatase based on green synthesized carbon dots and MnO_2 nanosheets. Talanta. 2017;165:136–42.
36. Niu N, Ma Z, He F, Li S, Li J, Liu S, et al. Preparation of carbon dots for cellular imaging by the molecular aggregation of cellulolytic enzyme lignin. Langmuir. 2017;33:5786–95.
37. Miao X, Qu D, Yang D, Nie B, Zhao Y, Fan H, et al. Synthesis of carbon dots with multiple color emission by controlled graphitization and surface functionalization. Adv Mater. 2018;30:1704740.
38. Sun S, Zhang L, Jiang K, Wu A, Lin H. Toward high-efficient red emissive carbon dots: facile preparation, unique properties, and applications as multifunctional theranostic agents. Chem Mater. 2016;28:8659–68.
39. Atchudan R, Edison TNJI, Sethuraman MG, Lee YR. Efficient synthesis of highly fluorescent nitrogen-doped carbon dots for cell imaging using unripe fruit extract of Prunus mume. Appl Surf Sci. 2016;384:432–41.
40. Jiang X, Shi Y, Liu X, Wang M, Song P, Xu F, et al. Synthesis of nitrogen-doped lignin/DES carbon quantum dots as a fluorescent probe for the detection of $Fe3^+$ ions. Polymers-Basel. 2018;10:1282.
41. Li LL, Ji J, Fei R, Wang CZ, Lu Q, Zhang JR, et al. A facile microwave avenue to electrochemiluminescent two-color graphene quantum dots. Adv Funct Mater. 2012;22:2971–9.
42. Zhang Q, Li W, Chen J, Wang F, Wang Y, Chen Y, et al. An ultrasensitive chemiluminescence turn-on assay for protease and inhibitor screening with a natural substrate. Chem Commun. 2013;49:3137–9.
43. Wang S, Cole IS, Zhao D, Li Q. The dual roles of functional groups in the photoluminescence of graphene quantum dots. Nanoscale. 2016;8:7449–58.
44. Li L, Yu B, You T. Nitrogen and sulfur co-doped carbon dots for highly selective and sensitive detection of Hg (II) ions. Biosens Bioelectron. 2015;74:263–9.
45. Lu S, Sui L, Liu J, Zhu S, Chen A, Jin M, et al. Near-infrared photoluminescent polymer-carbon nanodots with two-photon fluorescence. Adv Mater. 2017;29:1603443.
46. Ross PD, Subramanisn S. Thermodynamics of protein association reactions: forces contributing to stability. Biochemistry. 1981;20:3096–102.
47. Zhang L, Du J. A sensitive and label-free trypsin colorimetric sensor with cytochrome c as a substrate. Biosens Bioelectron. 2016;79:346–52.